Zitierweise: *Angew. Chem. Int. Ed.* **2024**, e202404527
doi.org/10.1002/anie.202404527

Low-Valent Compounds

Mercury-Group 13 Metal Covalent Bonds: A Systematic Comparison of Aluminyl, Gallyl and Indyl Metallo-ligands

*Liam P. Griffin, Mathias A. Ellwanger, Agamemnon E. Crumpton, Matthew M. D. Roy, Andreas Heilmann, and Simon Aldridge**

Abstract: Bimetallic compounds containing direct metal-group 13 element bonds have been shown to display unprecedented patterns of cooperative reactivity towards small molecules, which can be influenced by the identity of the group 13 element. In this context, we present here a systematic appraisal of group 13 metallo-ligands of the type $[(NON)E]^-$ (NON = 4,5-bis(2,6-di*iso*propylanilido)-2,7-di-tert-butyl-9,9-dimethylxanthene) for E = Al, Ga and In, through a comparison of structural and spectroscopic parameters associated with the *trans* L or X ligands in linear d^{10} complexes of the types LM{E(NON)} and XM′{E(NON)}. These studies are facilitated by convenient syntheses (from the In(I) precursor, InCp) of the potassium indyl species $[\{K(NON)In\}\cdot KCp]_n$ (**1**) and $[(18\text{-crown-6})_2K_2Cp]$ [(NON)In] (**1′**), and lead to the first structural characterisation of Ag–In and Hg–E (E = Al, In) covalent bonds. The resulting structural, spectroscopic and quantum chemical probes of Ag/Hg complexes are consistent with markedly stronger σ-donor capabilities of the aluminyl ligand, $[(NON)Al]^-$, over its gallium and indium counterparts.

Introduction

Bimetallic compounds featuring metals of different electronic character have received significant recent attention, not least due to their potential for the activation of small molecules in cooperative fashion. Systems featuring direct metal–metal bonds have featured heavily in such studies, with the proximity of the two metal centres, and the electronic perturbation brought about by the covalent interaction, helping to enable novel patterns of reactivity not accessible to either metal in isolation.[1] One class of bimetallic compound of this sort are systems featuring a late *d*-block metal (M) and a group 13 element (E) such as aluminium; with the combination of electron-rich and electron deficient metal centres allowing for the activation of kinetically inert substrates, such as C–H and C–F bonds, and CO_2.[2–4]

The study and use of 'metallo-ligands' featuring Group 13 metal centres has been greatly accelerated in recent years due to the development of nucleophilic sources of the $[EX_2]^-$ unit (typically as group 1 metal salts),[5] which allow access to M–Group 13 linkages via metathesis chemistry. Historically, anionic gallyl and boryl reagents were the first to be accessed (Figure 1);[6,7] since then $[BX_2]^-$ and $[GaX_2]^-$ ligands have been widely installed at metal centres from across the Periodic Table, with metal boryl complexes, for example, showing widespread synthetic utility in C–H borylation chemistry.[8] Subsequently, both thallyl and indyl systems were accessed by our group and the group of Coles, respectively,[9,10] with the most electropositive Group 13 element aluminium predictably being the last to yield tractable systems of the type $[EX_2]^-$.[11,12] As such, aluminyl and indyl metalloligands have been much less widely applied than their boryl and gallyl equivalents;[2,13,14] to our knowledge, no examples of covalently bound metal thallyl complexes currently exist.

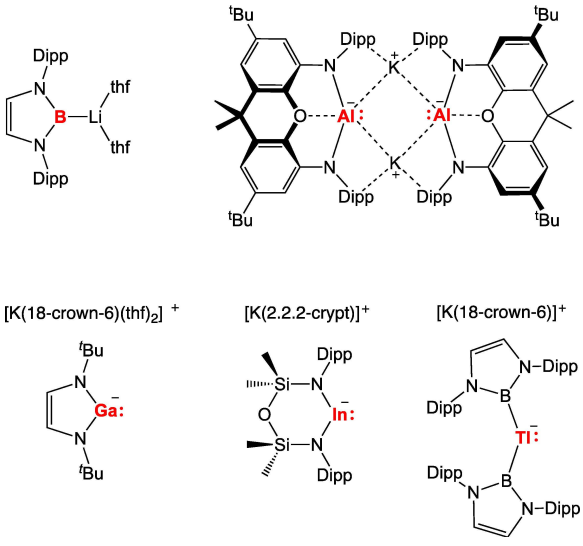

Figure 1. Early examples of trielyl anions relevant to the current study.

[*] L. P. Griffin, Dr. M. A. Ellwanger, A. E. Crumpton, Dr. M. M. D. Roy, Dr. A. Heilmann, Prof. S. Aldridge
Inorganic Chemistry Laboratory, Department of Chemistry, University of Oxford
South Parks Road, Oxford, OX1 3QR (UK)
E-mail: simon.aldridge@chem.ox.ac.uk

© 2024 The Authors. Angewandte Chemie published by Wiley-VCH GmbH. This is an open access article under the terms of the Creative Commons Attribution License, which permits use, distribution and reproduction in any medium, provided the original work is properly cited.

© 2024 The Authors. Angewandte Chemie published by Wiley-VCH GmbH

While a number of supporting ligand frameworks have been employed to stabilize anionic E(I) systems, systematic comparison of their behaviour as metallo-ligands as a function of the Group 13 metal (i.e. E = Al, Ga, In) has proved difficult due to the absence of a contiguous set of identically-supported systems. With this in mind, we sought a convenient source of the $[(NON)In]^-$ anion (NON = 4,5-bis(2,6-di*iso*propylanilido)-2,7-di-tert-butyl-9,9-dimethylxanthene), so that its chemistry as a metallo-ligand could be systematically compared with that of its previously reported aluminium and gallium congeners.[11a] These studies are reported here.

Results and Discussion

In contrast to previously reported methodologies for the synthesis of group 13 systems of the type $[EX_2]^-$ (which largely rely on the reduction of E^{III} halide precursors),[11g] we hypothesised that the more readily available nature of E^I precursors might offer an alternative metathesis approach for the heavier group 13 metals. With this in mind, we examined InCp as a convenient In(I) source,[15] aiming to use the reaction with K_2[NON] to access the potassium salt of the indyl anion, $[K\{(NON)In\}]_n$, and precipitate the sparingly soluble KCp by-product. In practice, this reaction proceeds rapidly, leading to the formation of a bright yellow solution, followed by immediate precipitation of a yellow microcrystalline material. Some of the crystalline material was of sufficient quality for single crystal X-ray diffraction studies, although due to relatively rapid crystallisation, the data obtained can only be used to establish connectivity. The structure of $[\{K(NON)In\}\cdot KCp]_n$, **1** (Figure 2), confirms that In(I) has been assimilated by the NON framework via substitution of the cyclopentadienyl ligand. However, the KCp co-product, rather than precipitating out of the benzene reaction solvent, has been retained, resulting in a coordination polymer in which $[(NON)In]^-$ fragments are bridged by potassium arene interactions involving both the Cp and NON fragments.

1 is resolutely insoluble in compatible solvents (but can act as a viable source of the $[(NON)In]^-$ unit in situ, see below). With the aim of generating a more tractable derivative, however, two equivalents of 18-crown-6 were added, leading to the formation of a related species **1′**, featuring discrete $[(18\text{-crown-6})K(\mu_2\text{-}\eta^5,\eta^5\text{-}C_5H_5)K(18\text{-crown-6})]^+$ and $[(NON)In]^-$ ions.[10] Crystallization from *ortho*-difluorobenzene yielded single crystals suitable for X-ray crystallography (Figure 2), and **1′** could also be characterised in solution by multinuclear NMR spectroscopy. The KCp by-product is again retained, this time in the form of the crown ether inverse-sandwich cation $[(18\text{-crown-6})K(\mu_2\text{-}\eta^5,\eta^5\text{-}C_5H_5)K(18\text{-crown-6})]^+$. No close K···In contacts are observed in the solid state.

With a complete set of NON-stabilised aluminyl, gallyl and indyl systems in hand, complexation studies were targeted to give systematic insight into their electronic structure, and (in particular) to probe their relative capabilities as σ-donor metallo-ligands. With a view to minimising the complicating influence of steric factors, we targeted linear d^{10} metal complexes of the types LAgE(NON) and XHgE(NON). In the former case, the aluminyl and gallyl complexes (^{t}Bu$_3$P)AgAl(NON) and (^{t}Bu$_3$P)AgGa(NON) have previously been reported by us,[2l] and so (^{t}Bu$_3$P)AgIn(NON) was targeted for initial comparison, via the bond length and coupling constant associated with the Ag–P bond *trans* to the indyl ligand. Accordingly, the reaction of (^{t}Bu$_3$P)AgI with **1** in toluene leads to the immediate formation of a bright yellow solution, and a colourless precipitate. Single crystals of the product were obtained from hexane solution, and X-ray crystallography was exploited to confirm the identity of the silver indyl complex **2** (Figure 3 and Table 1). As such, this chemistry not only delivers the first example of a silver–indium covalent bond,[16] but also, confirms that KCp inclusion species **1** is able to react as a functional source of the indyl anion $[(NON)In]^-$.

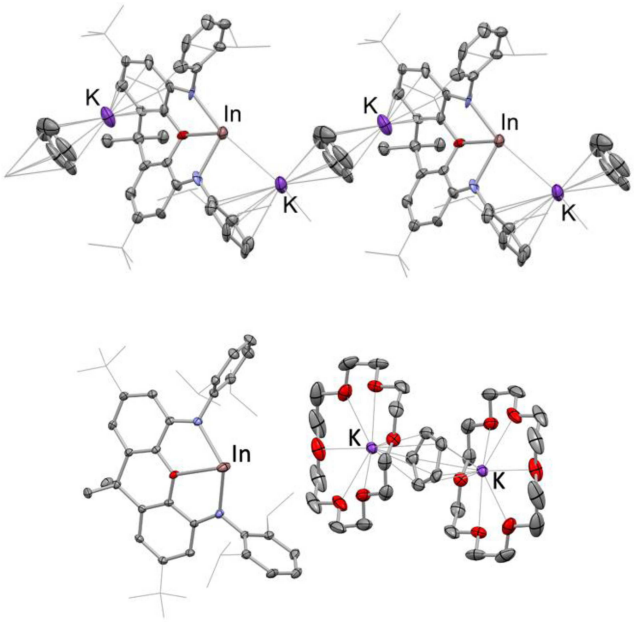

Figure 2. Molecular structures of $[\{K(NON)In\}\cdot KCp]_n$ (**1**; upper), and $[(18\text{-crown-6})K(\mu_2\text{-}\eta^5,\eta^5\text{-}C_5H_5)K(18\text{-crown-6})][(NON)In]$ (**1′**, lower) in the solid state as determined by X-ray crystallography. Hydrogen atoms and solvent molecules omitted, and selected groups shown in wireframe format for clarity; thermal ellipsoids set at the 40% level. Key bond lengths (Å) and angles (°): (for **1′**) In–N 2.342(4), 2.388(3); In–O 2.564(3); 120.7(1).

Table 1: NMR parameters and bond lengths for silver complexes (^{t}Bu$_3$P)AgM(NON) (M=Al, Ga, In).

M	*d*(Ag–P)/Å	δ_P/ppm	$^1J_{Ag\text{-}P}$/Hz
Al[2l]	–	58.9	161 (broad)[a]
Ga[2l]	2.4335(6)	65.4	278, 322
In	2.408(1)	68.5	334, 385

[a] Not resolved into ^{107}Ag and ^{109}Ag components due to quadrupolar broadening (^{27}Al; I = 5/2).

© 2024 The Authors. Angewandte Chemie published by Wiley-VCH GmbH

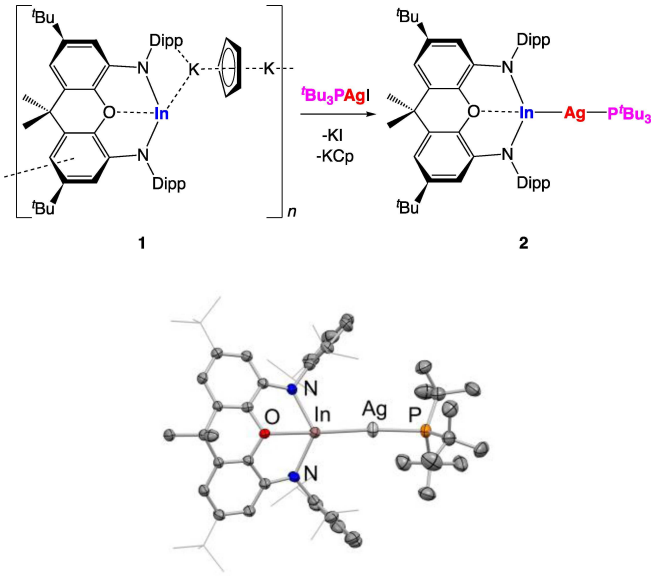

Figure 3. (upper) Synthesis and (lower) molecular structure of (^{t}Bu$_3$P)AgIn(NON), **2**, in the solid state as determined by X-ray crystallography. Hydrogen atoms and solvent molecules omitted, and selected groups shown in wireframe format for clarity; thermal ellipsoids set at the 40% level. Key bond lengths (Å) and angles (°): Ag–P 2.408(1), Ag–In 2.584(1), P–Ag–In 172.8(1).

The structure of **2** features a near linear P–Ag–In skeleton (172.8(1)°) in common with its gallyl counterpart;[21] the P–Ag bond *trans* to the metallo-ligand is somewhat shorter for the indyl compound (2.408(1) vs 2.4335(6) Å), implying that the heavier trielyl ligand has a weaker *trans* influence. Consistently, the $^1J_{AgP}$ coupling constants measured for **2** in benzene-d$_6$ solution (334 and 385 Hz for the ^{107}Ag and ^{109}Ag isotopes, respectively) are larger than those measured for (^{t}Bu$_3$P)AgGa(NON) (278 and 322 Hz).[21] For additional context, the corresponding $^1J_{AgP}$ coupling constant measured for (^{t}Bu$_3$P)AgAl(NON) is *much* lower (161 Hz) and is not resolved into ^{107}Ag/^{109}Ag components, presumably due to the quadrupolar nature of ^{27}Al. In addition, the ^{31}P NMR spectrum of the aluminyl complex in benzene-d$_6$ solution features 'free' ^{t}Bu$_3$P in equilibrium with the complex itself, consistent with the very high *trans* labilising ability of the [(NON)Al]$^-$ donor.[21] As such, we have been unable to crystallise (^{t}Bu$_3$P)AgAl(NON) from hydrocarbon solution. With this in mind, we turned instead to mercury(II) systems of the type XHgE(NON), hypothesizing that the X-ligand would be less labile, and would therefore allow us to structurally characterise (for the first time) a complete series of otherwise identical aluminyl, gallyl and indyl complexes.

While a number of supporting Hg–X systems were examined, most promising results were obtained for the borylmercury systems {(HCDippN)$_2$}BHgE(NON) (hitherto abbreviated as (boryl)HgE(NON)), for which (i) the bromide-bridged precursor [(boryl)Hg(μ-Br)]$_2$, is readily available;[17] and (ii) benchmarking of the [(NON)E]$^-$ ligands against other supporting group 13 ligand frameworks is also possible, by comparison with the known compounds (boryl)$_2$Hg and (boryl)Hg{Ga(NDippCH)$_2$}.[17]

Gallyl complex (boryl)HgGa(NON) is the most straightforward to synthesise and isolate (Scheme 1 and Figure 4). Addition of [(boryl)Hg(μ-Br)]$_2$ to a solution of K$_2$[(NON)Ga]$_2$ in benzene-d$_6$ leads to clean conversion to a new highly symmetrical species, (as judged by the presence of two Dipp CH$_3$ and one Dipp CH signals for the NON backbone in the ^{1}H NMR spectrum). Crystallisation from hexane yields a pale yellow crystalline material in 62% yield, which is stable at room temperature (in an inert atmosphere) and can be characterised by multinuclear NMR spectroscopy and elemental microanalysis. Moreover, X-ray diffraction could be employed to confirm the structure of the mercury gallyl product, (boryl)HgGa(NON), **4** (Figure 4 and Table 2). This compound offers direct comparison on another level with the diazabutadiene-supported gallyl complex (boryl)Hg{Ga(NDippCH)$_2$},[17] which was previously reported by us, and which also features the expected linear Ga–Hg–B skeleton.

The indium congener, (boryl)HgIn(NON) (**5**) can be synthesized in similar fashion from (boryl)Hg(μ-Br)]$_2$ and in situ generated **1**, with accompanying precipitation of KBr and KCp. ^{1}H NMR spectroscopy is consistent with a molecular structure in solution similar to that of **4**, and single crystals could also be obtained from hexane, although in lower yields (ca. 34%) due to slow decomposition of the product to indium metal. X-ray diffraction confirms the formation of complex **5** (Figure 4 and Table 2), which features the first example of an unsupported covalent bond between indium and mercury.

Finally, in the case of the more highly reducing aluminyl anion, the analogous synthetic approach is not as straightforward. Addition of [(boryl)BHg(μ-Br)]$_2$ to a solution of K$_2$[(NON)Al]$_2$ at room temperature leads to a complex ^{1}H NMR spectrum in which (boryl)$_2$Hg (**6**) can be observed

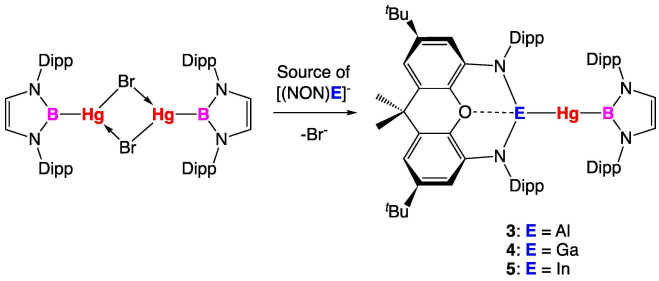

Scheme 1. Syntheses of (boryl)HgE(NON) complexes (E=Al (**3**), Ga (**4**), In (**5**)) from [(boryl)Hg(μ-Br)]$_2$.

Table 2: Structural parameters for mercury complexes (boryl)HgM(NON) (M=Al (**3**), Ga (**4**), In(**5**)) and related compounds.

M/E	*d*(Hg–B) (Å)	*d*(Hg–E) (Å)	r_{cov}(E) (Å)[19]	∠(B–Hg–M) (°)	δ_B (ppm)
3 Al	2.222(3)	2.594(1)	1.21	175.2(1)	75.7
4 Ga	2.181(4)	2.554(1)	1.22	179.5(1)	60.0
5 In	2.199(7)	2.709(1)	1.42	178.0(2)	54.4
6[17] B	2.150(3)	2.151(3)	0.84	179.0(1)	68.6
7[17] Ga	2.116(5)	2.476(1)	1.22	179.1(1)	56.4

© 2024 The Authors. Angewandte Chemie published by Wiley-VCH GmbH

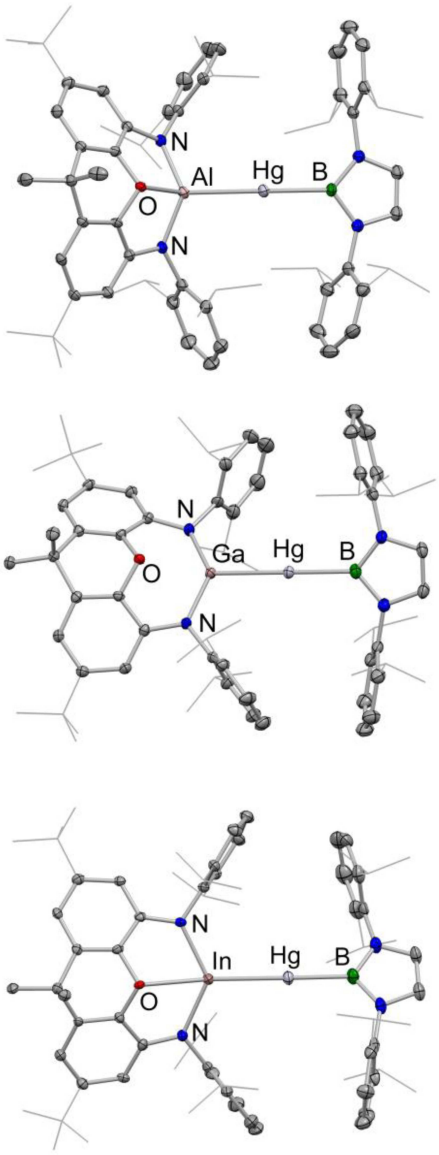

Figure 4. Molecular structures of **3** (upper), **4** (centre) and **5** (lower) in the solid state as determined by X-ray crystallography. Hydrogen atoms and solvent molecules omitted, and selected groups shown in wireframe format for clarity; thermal ellipsoids set at the 40% level. For key geometric data see Table 2.

as well as a major new species, the signals of which decrease steadily over the course of 1 h at room temperature. Use of the less reducing bis(aluminyl)-magnesium compound, $Mg\{Al(NON)\}_2$,[18] as the aluminyl source results in a cleaner product mixture (as judged by in situ ^{1}H NMR), with fewer unidentified side products, but decomposition of the major species still proceeds at room temperature. Reaction in a concentrated toluene solution at room temperature followed by immediate filtration and storage at 243 K, however, leads to the formation of single crystalline material, allowing for its investigation by X-ray crystallography. The solid-state structure determined confirms the formation of (boryl)HgAl(NON) (**3**; Figure 4 and Table 2), a mercury aluminyl complex, and the first structurally authenticated species containing a Hg–Al bond.

Structurally, complexes **3**–**5** feature very similar close-to-linear coordination geometries at the central metal centre, consistent with expectations for divalent mercury. The Hg–B bond lengths associated with the boryl group *trans* to the Al-, Ga- or In-based metallo-ligand are consistent with the hypothesis that the aluminyl ligand is a stronger σ-donor that its gallyl counterpart: the bond length is significantly longer for the aluminium donor (2.222(3) vs 2.181(4) Å). Unfortunately, the quality of the X-ray data in the case of indyl complex **5** renders any related analysis statistically insignificant. Interestingly, comparison of the structural data measured for the gallyl systems **4** and (boryl)Hg{Ga(NDippCH)$_2$} (**7**) reveals a markedly longer *trans* Hg–B bond in the case of **4** (2.181(4) vs. 2.116(5) Å) suggesting that the NON-ligand framework confers stronger donor properties on the group 13 donor than its diazabutadiene-derived analogue.

With a view to better understanding the structural properties of compounds **3**–**5** we also examined their electronic structures through a variety of quantum chemical techniques—carried out in each case on related model systems (**3***–**5***) in which the backbone ^{t}Bu groups of the NON ligands were replaced by Me for computational efficiency (see ESI for computational details). The geometries of the fully optimized structures agree closely with those measured crystallographically in the solid state, especially with respect to the Hg–B and Hg–E bond lengths. Quantum Theory of Atoms in Molecules (QT-AIM) and Electron Localization Function (ELF) methods were found to be the most informative probes of electronic structure; key data for model compounds **3***–**5*** are listed in Table 3 and shown pictorially (in the case of aluminyl compound **3***) in Figure 5.

In each of **3***–**5*** the HOMO and HOMO-3 are identified as σ-bonding orbitals extending across the whole of the E–Hg–B unit, with the HOMO-3 becoming the more dominant bonding component from Al to Ga to In. QT-AIM methods were also used to probe the nature of both Hg–B and Hg–E bonds. Conventional bond paths and Bond

Table 3: Selected (calculated) parameters relating to the Hg–E and Hg–B bonds in model mercury complexes **3***–**5***.

	Bond	ρ(r) (e Å^{-3})	$\nabla^2\rho$(r) (e Å^{-5})	WBI	Occupancy of ELF basin (e$^-$)
3*	Hg–B	0.100	−0.030	0.365	1.959 (37.6% Hg; 59.5% B)
	Hg–Al	0.059	0.013	0.545	1.862 (75.5% Hg; 21.8% Al)
4*	Hg–B	0.105	−0.054	0.466	1.939 (41.6% Hg; 55.9% B)
	Hg–Ga	0.069	0.004	0.516	1.919 (44.6% Hg; 54.1% Ga)
5*	Hg–B	0.105	−0.068	0.429	1.883 (44.0% Hg; 53.8% B)
	Hg–In	0.056	0.032	0.490	1.756 (40.8% Hg; 57.9% In)

© 2024 The Authors. Angewandte Chemie published by Wiley-VCH GmbH

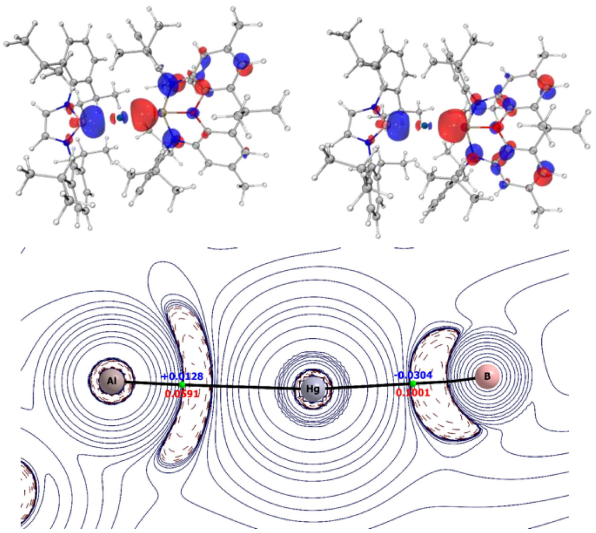

Figure 5. Analysis of bonding in model mercury aluminyl complex **3***: (upper) HOMO and HOMO-3 of **3***; (lower) Contour plot of the Laplacian of the electron density in the plane of the Al–Hg–B moiety from QT-AIM analysis: Bond Critical Points (BCPs) are shown in green, along with the electron density [$\rho(r)$] and Laplacian of the electron density [$\nabla^2\rho(r)$] at the Hg–Al and Hg–B bond critical points.

Critical Points (BCPs) were located for all Hg–E/Hg–B linkages (Figure 5). Analysis of both the electron density at the critical point $\rho(r)$ and its Laplacian $\nabla^2\rho(r)$, together with the associated kinetic and potential energy densities at the BCPs classify the Hg–B bonds as (polar) covalent and the Hg–E bonds as metallic (Table 3).[20] Comparisons of (i) the values of $\rho(r)$ for the Hg–B bonds (0.100, 0.105, 0.105 e Å^{-3}, for **3***, **4*** and **5***, respectively); (ii) the Wiberg Bond Indices (WBIs) for the Hg–B bonds (0.365, 0.466 and 0.429) and (iii) the Bader charges at mercury (−0.44, −0.06 and −0.01) and all imply that the aluminyl ligand in **3*** is the strongest σ-donor of the three metallo-ligands. ELF calculations were also used to analyse the electron density in the regions between the Hg and E/B nuclei, and provide further corroboration that the $[(NON)Al]^-$ system is the strongest σ-donor of the three. As such, the Hg–B bond is more polarized towards boron, and the Hg–E bond *significantly* more polarized towards mercury in the case of (model) aluminyl complex **3*** (i.e. for E = Al; Table 3).

Conclusion

Facile syntheses of sources of the indyl anion $[(NON)In]^-$ are reported, and their utility in the construction of In–Ag and In–Hg covalent bonds has been demonstrated. In both cases the corresponding aluminium and gallium congeners have also been synthesised, thereby providing two complete series showcasing the three metallo-ligands $[(NON)E]^-$ (E = Al, Ga, In) in which the supporting ligand scaffold is unchanged. Crystallographic, spectroscopic and quantum chemical comparisons of these complexes provide insight into how the geometric and electronic structure of these ligands varies as group 13 is descended, and also allows for comparison with metallo-ligands featuring alternative supporting frameworks. In this regard the NON-supported systems are thought to be stronger σ-donors than their diazabutadiene-derived analogues, with $[(NON)Al]^-$ offering the most potent σ-donation; consistent with aluminium's position as the most electropositive metal of Group 13.[21]

Supporting Information

Included in the Supporting Information are synthetic and characterizing data relating to new compounds, representative spectra, and details of quantum chemical calculations and X-ray crystallography. CIFs are available from the CCDC (2334028–2334034).[21–46]

Acknowledgements

We thank the EPSRC Centre for Doctoral Training in Inorganic Chemistry for Future Manufacturing (OxICFM, EP/S023828/1, studentships to L.P.G. and A.E.C.), the Leverhulme Trust (studentship to A.H.) and the Alexander von Humboldt Foundation for funding (Feodor Lynen postdoctoral research fellowship to M. A. E.).

Conflict of Interest

The authors declare no conflict of interest.

Data Availability Statement

The data that support the findings of this study are available in the supplementary material of this article.

Keywords: group 13 elements · low valent compounds · aluminyl · gallyl · indyl · mercury

[1] For reviews of bimetallics in small molecule activation see, for example: a) B. G. Cooper, J. W. Napoline, C. M. Thomas, *Catal. Rev. Sci. Eng.* **2012**, *54*, 1–40; b) N. P. Mankad, *Chem. Eur. J.* **2016**, *22*, 5822–5829; c) J. Takaya, *Chem. Sci.* **2021**, *12*, 1964–1981; d) M. T. Whited, *Dalton Trans.* **2021**, *50*, 16443–16450.

[2] Examples of transition metal-aluminium bimetallics featuring an X-type group 13 ligand: a) R. A. Fischer, T. Priermeier, *Organometallics* **1994**, *13*, 4306–4314; b) B. N. Anand, I. Krossing, H. Nöth, *Inorg. Chem.* **1997**, *36*, 1979–1981; c) I. M. Riddlestone, J. Urbano, N. D. Phillips, M. J. Kelly, D. Vidovic, J. I. Bates, R. Taylor, S. Aldridge, *Dalton Trans.* **2013**, *42*, 249–258; d) J. Takaya, N. Iwasawa, *J. Am. Chem. Soc.* **2017**, *139*, 6074–6077; e) N. Hara, T. Saito, K. Semba, N. Kuriakose, H. Zheng, S. Sakaki, Y. Nakao, *J. Am. Chem. Soc.* **2018**, *140*, 7070–7073; f) J. Hicks, A. Mansikkamäki, P. Vasko, J. M. Goicoechea, S. Aldridge, *Nat. Chem.* **2019**, *11*, 237–241; g) S. Morisako, S. Watanabe, S. Ikemoto, S. Muratsugu, M. Tada, M. Yamashita, *Angew. Chem. Int. Ed.* **2019**, *58*, 15031–15035;

© 2024 The Authors. Angewandte Chemie published by Wiley-VCH GmbH

h) K. Sugita, M. Yamashita, *Chem. Eur. J.* **2020**, *26*, 4520–4523; i) I. Fujii, K. Semba, Q.-Z. Li, S. Sakaki, Y. Nakao, *J. Am. Chem. Soc.* **2020**, *142*, 11647; j) R. Seki, N. Hara, T. Saito, Y. Nakao, *J. Am. Chem. Soc.* **2021**, *143*, 6388–6394; k) H. Y. Liu, R. J. Schwamm, M. S. Hill, M. F. Mahon, C. F. McMullin, N. A. Rajabi, *Angew. Chem. Int. Ed.* **2021**, *60*, 14390–14393; l) C. McManus, J. Hicks, X. Cui, L. Zhao, G. Frenking, J. M. Goicoechea, S. Aldridge, *Chem. Sci.* **2021**, *12*, 13458–13468; m) B. J. Graziano, M. V. Vollmer, C. C. Lu, *Angew. Chem. Int. Ed.* **2021**, *60*, 15087–15094; n) M. M. D. Roy, J. Hicks, P. Vasko, A. Heilmann, A.-M. Baston, J. M. Goicoechea, S. Aldridge, *Angew. Chem. Int. Ed.* **2021**, *60*, 22301–22306; o) M. J. Evans, G. H. Iliffe, S. E. Neale, C. L. McMullin, J. R. Fulton, M. D. Anker, M. P. Coles, *Chem. Commun.* **2022**, *58*, 10091–10094; p) C. McManus, A. E. Crumpton, S. Aldridge, *Chem. Commun.* **2022**, *58*, 8274–8277.

[3] Transition metal-aluminium bimetallics featuring a L-type group 13 ligand have a longer historical precedent. For a review of early work in this area see: R. A. Fischer, J. Weiß, *Angew. Chem. Int. Ed.* **1999**, *38*, 2830–2850.

[4] For a review of transition metal-aluminium bimetallics featuring a Z-type group 13 ligand see: R. C. Cammarota, L. J. Clouston, C. C. Lu, *Coord. Chem. Rev.* **2017**, *334*, 100–111.

[5] See for example, M. Assay, C. Jones, M. Driess, *Chem. Rev.* **2011**, *111*, 354–396.

[6] Ga: a) E. S. Schmidt, A. Jockisch, H. Schmidbaur, *J. Am. Chem. Soc.* **1999**, *121*, 9758–9759. See also b) R. J. Baker, R. D. Farley, C. Jones, M. Kloth, D. M. Murphy, *J. Chem. Soc. Dalton Trans.* **2002**, 3844–3850; c) I. L. Fedushkin, A. N. Lukoyanov, G. K. Fukin, S. Y. Ketkov, M. Hummert, H. Schumann, *Chem. Eur. J.* **2008**, *14*, 8465–8468.

[7] B: a) Y. Segawa, M. Yamashita, K. Nozaki, *Science* **2006**, *314*, 113–115. See also b) Y. Segawa, Y. Suzuki, M. Yamashita, K. Nozaki, *J. Am. Chem. Soc.* **2008**, *130*, 16069–16079; c) W. Lu, H. Hu, Y. Li, R. Ganguly, R. Kinjo, *J. Am. Chem. Soc.* **2016**, *138*, 6650–6661; d) A.-F. Pécharman, A. L. Colebatch, M. S. Hill, C. L. McMullin, M. F. Mahon, C. Weetman, *Nat. Commun.* **2017**, *8*, 15022; e) L. Weber, *Eur. J. Inorg. Chem.* **2017**, 3461–3488.

[8] a) I. A. I. Mkhalid, J. H. Barnard, T. B. Marder, J. M. Murphy, J. F. Hartwig, *Chem. Rev.* **2010**, *110*, 890–931; b) I. F. Yu, J. W. Wilson, J. F. Hartwig, *Chem. Rev.* **2023**, *123*, 11619–11663.

[9] Tl: A. V. Protchenko, D. Dange, J. R. Harmer, C. Y. Tang, A. D. Schwarz, M. J. Kelly, N. Phillips, R. Tirfoin, K. H. Birjkumar, C. Jones, N. Kaltsoyannis, P. Mountford, S. Aldridge, *Nat. Chem.* **2014**, *6*, 315–319.

[10] In: R. J. Schwamm, M. D. Anker, M. Lein, M. P. Coles, C. M. Fitchett, *Angew. Chem. Int. Ed.* **2018**, *57*, 5885–5887.

[11] Al: a) J. Hicks, P. Vasko, J. M. Goicoechea, S. Aldridge, *Nature* **2018**, *557*, 92–95. See also: b) R. J. Schwamm, M. D. Anker, M. Lein, M. P. Coles, *Angew. Chem. Int. Ed.* **2019**, *58*, 1489–1493; c) J. Hicks, P. Vasko, J. M. Goicoechea, S. Aldridge, *J. Am. Chem. Soc.* **2019**, *141*, 11000–11003; d) S. Kurumada, S. Takamori, M. Yamashita, *Nat. Chem.* **2020**, *12*, 36–39; e) R. J. Schwamm, M. P. Coles, M. S. Hill, M. F. Mahon, C. L. McMullin, N. A. Rajabi, A. S. S. Wilson, *Angew. Chem. Int. Ed.* **2020**, *59*, 3928–3932; f) K. Koshino, R. Kinjo, *J. Am. Chem. Soc.* **2020**, *142*, 9057–9062; g) S. Grams, J. Eyselein, J. Langer, C. Färber, S. Harder, *Angew. Chem. Int. Ed.* **2020**, *59*, 15982–15986; h) S. Grams, J. Mai, J. Langer, S. Harder, *Organometallics* **2022**, *41*, 2862–2867; i) G. Feng, K. L. Chan, Z. Lin, M. Yamashita, *J. Am. Chem. Soc.* **2022**, *144*, 22662–22668; j) C. Yan, R. Kinjo, *Angew. Chem. Int. Ed.* **2022**, *61*, e202211800; k) R. A. Jackson, A. J. R. Matthews, P. Vasko, M. F. Mahon, J. Hicks, D. Liptrot, *Chem. Commun.* **2023**, *59*, 5277–5280; l) D. Sarkar, P. Vasko, A. F. Roper, M. M. D. Roy, A. E. Crumpton, L. P. Griffin, C. Bogle, S. Aldridge, *J. Am. Chem. Soc.* **2024**, ASAP (DOI: 10.1021/jacs.4c00376).

[12] For recent reviews of aluminyl and related chemistry, see for example: a) K. Hobson, C. J. Carmalt, C. Bakewell, *Chem. Sci.* **2020**, *11*, 6942–6956; b) J. Hicks, P. Vasko, J. M. Goicoechea, S. Aldridge, *Angew. Chem. Int. Ed.* **2021**, *60*, 1702–1711; c) M. P. Coles, M. J. Evans, *Chem. Commun.* **2023**, *59*, 503–519.

[13] a) G. J. Irvine, M. J. G. Lesley, T. B. Norman, N. C. Norman, C. R. Rice, E. G. Robins, W. R. Roper, G. R. Whittell, L. J. Wright, *Chem. Rev.* **1998**, *98*, 2685–2722; b) H. Braunschweig, R. D. Dewhurst, A. Schneider, *Chem. Rev.* **2010**, *110*, 3924–3957.

[14] For a review of the coordination chemistry of gallyl systems, see for example: R. J. Baker, C. Jones, *Coord. Chem. Rev.* **2005**, *249*, 1857–1869.

[15] E. O. Fischer, H. P. Hofmann, *Angew. Chem.* **1957**, *69*, 639–640.

[16] For an example of an In/Ag donor/acceptor interaction see: M. Lichtenthaler, F. Stahl, D. Kratzert, L. Heidinger, E. Schleicher, J. Hamann, D. Himmel, S. Weber, I. Krossing, *Nat. Commun.* **2015**, *6*, 8288.

[17] A. V. Protchenko, D. Dange, A. D. Schwarz, C. Y. Tang, N. Phillips, P. Mountford, C. Jones, S. Aldridge, *Chem. Commun.* **2014**, *50*, 3841–3844.

[18] L. P. Griffin, M. Ellwanger, J. Clarke, A. F. Roper, A. Heilmann, S. Aldridge, *Angew. Chem. Int. Ed.* **2024**, *63*, 3202405053.

[19] B. Cordero, V. Gómez, A. E. Platero-Prats, M. Revés, J. Echeverría, E. Cremades, F. Barragán, S. Alvarez, *Dalton Trans.* **2008**, 2832–2838.

[20] R. Bianchi, G. Gervasio, D. Marabello, *Inorg. Chem.* **2000**, *39*, 2360–2366.

[21] Deposition numbers 2334028–2334034 contain the supplementary crystallographic data for this paper. These data are provided free of charge by the joint Cambridge Crystallographic Data Centre and Fachinformationszentrum Karlsruhe Access Structures service.

[22] C. A. Cruz, D. J. H. Emslie, L. E. Harrington, J. F. Britten, C. M. Robertson, *Organometallics* **2007**, *26*, 692–701.

[23] R. G. Goel, A. L. Beauchamp, *Inorg. Chem.* **1983**, *22*, 395–400.

[24] J. Cosier, A. M. Glazer, *J. Appl. Crystallogr.* **1986**, *19*, 105–107.

[25] CrysAlisPro v.1.171.42.70a, Agilent Technologies, 2011.

[26] G. M. Sheldrick, *Acta Crystallogr.* **2015**, *A71*, 3–8.

[27] G. M. Sheldrick, *Acta Crystallogr.* **2015**, *C71*, 3–8.

[28] O. V. Dolomanov, L. J. Bourhis, R. J. Gildea, J. A. K. Howard, H. Puschmann, *J. Appl. Crystallogr.* **2009**, *42*, 339–341.

[29] Y. Zhao, D. G. Truhlar, *Theor. Chem. Acc.* **2008**, *120*, 215–241.

[30] F. Weigend, R. Ahlrichs, *Phys. Chem. Chem. Phys.* **2005**, *7*, 3297–3305.

[31] S. Grimme, J. Antony, S. Ehrlich, H. Krieg, *J. Chem. Phys.* **2010**, *132*, 154104.

[32] M. J. Frisch, G. W. Trucks, H. B. Schlegel, G. E. Scuseria, M. A. Robb, J. R. Cheeseman, G. Scalmani, V. Barone, G. A. Petersson, H. Nakatsuji, X. Li, M. Caricato, A. V. Marenich, J. Bloino, B. G. Janesko, R. Gomperts, B. Mennucci, H. P. Hratchian, J. V. Ortiz, A. F. Izmaylov, J. L. Sonnenberg, D. Williams-Young, F. Ding, F. Lipparini, F. Egidi, J. Goings, B. Peng, A. Petrone, T. Henderson, D. Ranasinghe, V. G. Zakrzewski, J. Gao, N. Rega, G. Zheng, W. Liang, M. Hada, M. Ehara, K. Toyota, R. Fukuda, J. Hasegawa, M. Ishida, T. Nakajima, Y. Honda, O. Kitao, H. Nakai, T. Vreven, K. Throssell, J. A. Montgomery Jr., J. E. Peralta, F. Ogliaro, M. J. Bearpark, J. J. Heyd, E. N. Brothers, K. N. Kudin, V. N. Staroverov, T. A. Keith, R. Kobayashi, J. Normand, K. Raghavachari, A. P. Rendell, J. C. Burant, S. S. Iyengar, J. Tomasi, M. Cossi, J. M. Millam, M. Klene, C. Adamo, R. Cammi, J. W. Ochterski, R. L. Martin, K. Morokuma, O.

© 2024 The Authors. Angewandte Chemie published by Wiley-VCH GmbH

Farkas, J. B. Foresman, D. J. Fox, *Gaussian 16, Revision C.01*, Gaussian, Inc., Wallingford CT **2016**.
[33] E. van Lenthe, J. G. Snijders, E. J. Baerends, *J. Chem. Phys.* **1996**, *105*, 6505–6516.
[34] J. D. Rolfes, F. Neese, D. A. Pantazis, *J. Comput. Chem.* **2020**, *41*, 1842–1849.
[35] D. A. Pantazis, F. Neese, *J. Chem. Theory Comput.* **2009**, *5*, 2229–2238.
[36] D. A. Pantazis, X. Y. Chen, C. R. Landis, F. Neese, *J. Chem. Theory Comput.* **2008**, *4*, 908–911.
[37] D. A. Pantazis, F. Neese, *Theor. Chem. Acc.* **2012**, *131*, 1292.
[38] D. A. Pantazis, F. Neese, *J. Chem. Theory Comput.* **2011**, *7*, 677–684.
[39] F. Weigend, *Phys. Chem. Chem. Phys.* **2006**, *8*, 1057–1065.
[40] F. Neese, F. Wennmohs, U. Becker, C. Riplinger, *J. Chem. Phys.* **2020**, *152*, 224108.
[41] NBO 7.0., E. D. Glendening, J, K. Badenhoop, A. E. Reed, J. E. Carpenter, J. A. Bohmann, C. M. Morales, P. Karafiloglou, C. R. Landis, F. Weinhold, Theoretical Chemistry Institute, University of Wisconsin, Madison **2018**.
[42] AIMAll (Version 19.10.12), T. A. Keith, TK Gristmill Software, Overland Park KS, USA **2019** (aim.tkgristmill.com).
[43] T. Lu, F. Chen, *J. Comput. Chem.* **2012**, *33*, 580–592.
[44] B. Silvi, A. Savin, *Nature* **1994**, *371*, 683–686.
[45] E. F. Pettersen, T. D. Goddard, C. C. Huang, G. S. Couch, D. M. Greenblatt, E. C. Meng, T. E. Ferrin, *J. Comput. Chem.* **2004**, *25*, 1605–1612.
[46] R. Bianchi, G. Gervasio, D. Marabello, *Inorg. Chem.* **2000**, *39*, 2360–2366.

Manuscript received: March 5, 2024
Accepted manuscript online: March 28, 2024
Version of record online: ■■, ■■

© 2024 The Authors. Angewandte Chemie published by Wiley-VCH GmbH

Forschungsartikel

Low-Valent Compounds

L. P. Griffin, M. A. Ellwanger,
A. E. Crumpton, M. M. D. Roy,
A. Heilmann, S. Aldridge* — **e202404527**

Mercury-Group 13 Metal Covalent Bonds: A Systematic Comparison of Aluminyl, Gallyl and Indyl Metallo-ligands

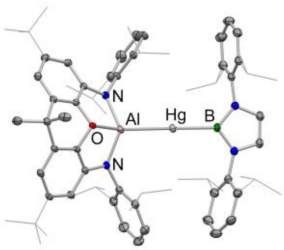

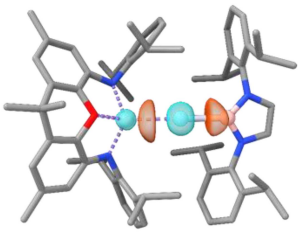

Aided by the syntheses of potassium indyl reagents, access is possible for the first time to a complete series of metal-trielyl complexes featuring the same xanthene-derived NON-framework. Analysis of mercury compounds of the type (boryl)HgE(NON) (E=Al, Ga, In) by structural, spectroscopic and theoretical methods shows that the aluminyl metallo-ligand $[(NON)Al]^-$ is the most potent σ-donor.

© 2024 The Authors. Angewandte Chemie published by Wiley-VCH GmbH